

Demonstration by ^2H ENDOR Spectroscopy that *myo*-Inositol Binds via an Alkoxide Bridge to the Mixed-Valent Diiron Center of *myo*-Inositol Oxygenase

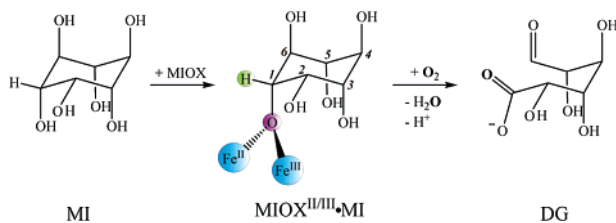
Sun Hee Kim,[†] Gang Xing,[‡] J. Martin Bollinger, Jr.,^{*,‡,§} Carsten Krebs,^{*,‡,§} and Brian M. Hoffman^{*,†}

Department of Chemistry, Northwestern University, Evanston, Illinois 60208-3113, Department of Biochemistry and Molecular Biology, and Department of Chemistry, The Pennsylvania State University, University Park, Pennsylvania 16802

Received May 23, 2006; E-mail: jmb21@psu.edu; ckrebs@psu.edu; bmh@northwestern.edu

myo-Inositol oxygenase (MIOX), a recent addition to the non-heme diiron oxygenase enzyme family, uses its dinuclear iron cluster to activate O_2 for cleavage of cyclohexane-(1,2,3,5/4,6-hexa)-ol (*myo*-inositol, MI) to D-glucuronate (DG), a four electron oxidation (Scheme 1).^{1–3} A recent study^{4–6} showed that the mixed-

Scheme 1



valent, $\text{Fe}_2(\text{II/III})$ form of the cofactor, rather than the $\text{Fe}_2(\text{II/II})$ form used by all other non-heme diiron oxygenases characterized prior to MIOX, activates O_2 to generate DG. It was further speculated that MI binds as an alkoxide bridge to the diiron(II/III) cluster (shown in Scheme 1 in one possible binding mode) to activate the substrate for abstraction of H1 by a formally (superoxo)-diiron(III/III) intermediate. Determination of the structure of MI-bound MIOX ($\text{MIOX}^{\text{II/III}}\cdot\text{MI}$), in particular whether the substrate does indeed coordinate to the cluster and, if so, the precise binding mode, is essential for establishing the mechanistic pathway employed by MIOX. Here, we use ^2H ENDOR spectroscopy both to demonstrate that MI binds via an alkoxide bridge between the two Fe ions and to determine the orientation of the closest C–H bond relative to the diiron core.

$\text{MIOX}^{\text{II/III}}\cdot\text{MI}$ exhibits an axial EPR signal characteristic of an antiferromagnetically coupled, mixed-valent diiron center, with $g = [1.95, 1.81, 1.81]$.⁴ Figure 1 displays a 2D field-frequency plot comprising ^2H Mims ENDOR⁷ spectra collected⁸ at multiple fields across the EPR envelope on a sample prepared with uniformly C(1–6) deuterium-labeled MI ($[\text{C}^2\text{H}]_6\text{-MI}$).⁹ At all fields, the breadth of the pattern is determined by the $\nu(\pm)$ peaks of a hyperfine-split doublet from a strongly coupled deuteron ($^2\text{H}_a$);¹⁰ the peaks are sufficiently broad that there is no evidence of the additional quadrupole splitting of each peak expected for ^2H ($I = 1$). The strong variation of the hyperfine splitting with field indicates that the coupling is quite anisotropic. At intermediate fields, doublets from two additional, less strongly coupled deuterons ($^2\text{H}_b$, $^2\text{H}_c$) can also be seen: at $g = 1.85$, $A(^2\text{H}_a) \sim 2.1$ MHz, $A(^2\text{H}_b) \sim 1.2$ MHz, and $A(^2\text{H}_c) \sim 0.6$ MHz. None of the three deuterons show resolved quadrupole splittings at any field.

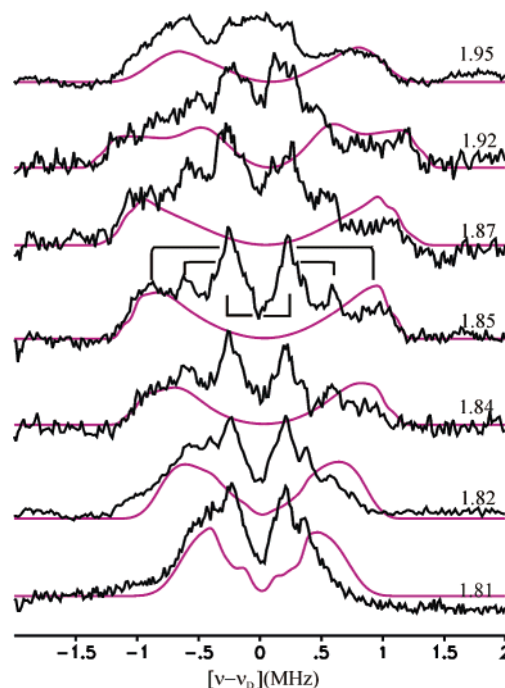


Figure 1. ^2H Mims ENDOR spectra of $\text{MIOX}^{\text{II/III}}\cdot[\text{C}^2\text{H}]_6\text{-MI}$. Brackets in the central spectrum ($g = 1.85$) indicate peaks from $^2\text{H}_{a-c}$. Conditions: $T = 2$ K; m.w. frequency = 34.76 GHz; $\pi/2 = 52$ ns; r.f. pulse length = 60 μs ; $\tau = 300$ ns; repetition rate = 50 Hz; and spectral resolution, 256 points; 30 samplings per point; 20–40 scans per point. Simulation parameters: $g = [1.95, 1.81, 1.81]$; $A = [-2.1, -0.5, 2.6]$ MHz, $[\alpha, \beta, \gamma] = [0, 55, 0]$; $P = [-0.045, -0.045, 0.09]$ MHz, $[\beta_a, \alpha_a] = [61, 83]$; EPR line width = 300 MHz; and ENDOR line width = 70 kHz.

Analysis of the 2D ENDOR pattern for $^2\text{H}_a$ provides the key to the geometry of the bound substrate. The 2D field-frequency pattern for $^2\text{H}_a$ could be reproduced by simulations that employed a hyperfine tensor with negligible isotropic coupling and an almost completely rhombic anisotropic interaction, $\mathbf{A}(^2\text{H}_a) = \mathbf{T}\mathbf{1} = [-2.3, -0.4, 2.7]$ MHz. As has been shown,^{11,12} such a tensor is characteristic of a nucleus that lies nearly equidistant from the two Fe ions: such a “bridging” ^2H is characterized by a nearly rhombic hyperfine tensor, $\mathbf{A} \sim \mathbf{T} \sim [-T, 0, T]$, where the $T_2 \sim 0$ principal axis lies normal to the $\text{Fe}(\text{H})\text{Fe}$ plane. Moreover, the large values for the principal components of $\mathbf{T}\mathbf{1}$ require that $^2\text{H}_a$ lies at a distance from the cluster that would be characteristic of a deuteron bonded to a carbon that also provides an alkoxide bridge. We, therefore, modeled the structure of a diiron center bridged by an MI alkoxide and used this model in conjunction with the data of Figure 1 to refine the structure of the center, as follows.

The net anisotropic interaction of a nucleus interacting with the $S = 1/2$ ground state of a spin-coupled, mixed-valent $\text{Fe}_2(\text{II/III})$

[†] Northwestern University.

[‡] Department of Biochemistry and Molecular Biology, The Pennsylvania State University.

[§] Department of Chemistry, The Pennsylvania State University.

center is taken as the weighted sum of the point-dipole interactions with the individual ions

$$\mathbf{T} = \frac{7}{3}\mathbf{T}^{\text{(III)}} - \frac{4}{3}\mathbf{T}^{\text{(II)}} \quad (1)$$

where $\frac{7}{3}$ and $-\frac{4}{3}$ are the spin-projection coefficients for the Fe(III) ($S = \frac{5}{2}$) and Fe(II) ($S = 2$) ions, respectively, and the \mathbf{T}^i are the uncoupled dipolar interactions between the ^2H and an individual iron ion Fe(i). For a given geometry of the diiron center, the tensor sum, \mathbf{T} , can be diagonalized to obtain an expression for the effective hyperfine tensor of the spin-coupled cluster system.^{11,12} We assumed an idealized equilateral Fe–O–Fe triangle with Fe–Fe distance ($d_{\text{Fe–Fe}}$) = 3.4 Å, as in mixed-valence methane monooxygenase hydroxylase,¹³ Fe–O distances ($r_{\text{Fe–O}}$) = 1.92 Å, tetrahedral geometry at O and C, and C–O and C– ^2H bond lengths ($d_{\text{O–C}}$ and $d_{\text{C–}^2\text{H}}$) of 1.43 and 1.1 Å, respectively;¹⁴ Figure 2 shows a portion of the model with O1 as bridge. To calculate \mathbf{T} , one needs the Fe(III)– $^2\text{H}_a$ distance and the angle between the Fe(III)– $^2\text{H}_a$ and Fe–Fe vectors, and these can be parametrically written in terms of the angle of rotation of the MI ring about the O–C1 bond, ϕ ; we adopt the convention, $\phi = 0$, for the symmetric geometry with the O–C1– $^2\text{H}_1$ plane orthogonal to the Fe–O1–Fe plane (Figure 2).

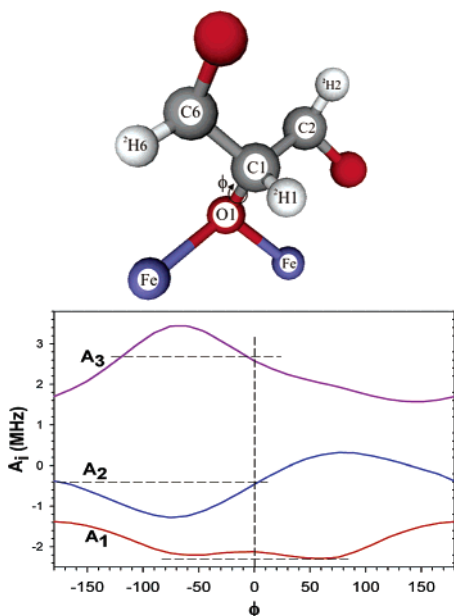


Figure 2. (Upper) Model of MI bound through O1 to the diiron cluster, drawn with $\phi = 0$ (see text) and so that $\phi > 0$ (arrow) rotates $^2\text{H}_1$ toward Fe(II). (Lower) Plot of $A_i(\phi) = \mathbf{T}_i(\phi)$. Horizontal dashed lines give $A_i(\text{H}_a)$, determined independently.

We calculated $\mathbf{T}(\phi)$ for all angles, and its principal values are plotted in Figure 2. The principal values for $A(^2\text{H}_a)$ determined by the independent fit to the 2D– ^2H pattern agree with the values predicted from the geometric model, $A(^2\text{H}_a) = \mathbf{T}(\phi = 0) = [-2.1, -0.5, 2.6]$ MHz, and the simulations based on these values match the experimental spectra well (Figure 1). The ^2H quadrupole tensor, \mathbf{P} , for $^2\text{H}_a$ likewise was parametrically written in terms of ϕ . \mathbf{P} for an aliphatic deuteron has axial symmetry with the unique value along the C– ^2H bond, $\mathbf{P} = [-P/2, -P/2, P]$; $P = e^2qQ/2 = 87$ kHz, as for C– ^2H of cyclohexane.¹⁵ However, inclusion of the quadrupole interaction has negligible influence on the simulations.

Examination of the model for MI binding further discloses that the partially resolved signals from $^2\text{H}_b$ and $^2\text{H}_c$ must arise from the C– ^2H adjacent to C_a – $^2\text{H}_a$ associated with the bridging oxygen.

To explore the structural constraints provided by these signals, we have considered models in which MI is in the chair conformation with either five axial or five equatorial OH substituents. We have considered only the C1, C2, and C6 oxygens for the bridging ligand, on the grounds that a C3–, C4–, or C5–O bridge is unlikely to be compatible with the postulated abstraction of H1 after addition of O₂ to the Fe(II) site.^{4–6} Furthermore, within the constraints provided by the available data, C2– and C6–O-bridged structures are indistinguishable: for both C2 and C6, the hydrogens bonded to the adjacent carbons would be either both axial or both equatorial. These models have been used to predict the anisotropic couplings to [$^2\text{H}_2, ^2\text{H}_6$] (O1 bridge) or [$^2\text{H}_1, ^2\text{H}_5(3)$] (O6(2) bridge), each with both possible assignments of the iron valencies. Preliminary comparisons of the experimental spectra and the predictions disfavor an equatorial O1 bridge and an axial O6(2) bridge.

The successful analysis of the $^2\text{H}_a$ ENDOR signals according to a structural model for the diiron center (Figure 2) thus shows that MI indeed binds to the mixed-valence diiron center of MIOX via a bridging alkoxide, while further analysis of the $^2\text{H}_b$ and $^2\text{H}_c$ has begun to reveal the full structure of the bound substrate. The model is completely consistent with the proposed initial steps of the catalytic mechanism: addition of O₂ to the cofactor Fe(II) ion and abstraction of H1.⁶ Further analysis and ENDOR experiments with specifically deuterated MI will reveal which carbon of MI provides the alkoxide bridge and the ring conformation in the complex.

Acknowledgment. This work was supported by the NIH (HL13531, B.M.H.), by Johnson and Johnson Corp., and by the Huck Institutes for the Life Sciences (JMB, G.X., C.K.).

Supporting Information Available: One figure that compares hyperfine tensors calculated for two ($d_{\text{Fe–Fe}}$). This material is available free of charge via the Internet at <http://pubs.acs.org>.

References

- Charalampous, F. C.; Lyras, C. *J. Biol. Chem.* **1957**, *228*, 1–13.
- Charalampous, F. C. *J. Biol. Chem.* **1959**, *234*, 220–227.
- Moskala, R.; Reddy, C. C.; Minard, R. D.; Hamilton, G. A. *Biochem. Biophys. Res. Commun.* **1981**, *99*, 107–113.
- Xing, G.; Hoffart, L. M.; Diao, Y.; Prabhu, K. S.; Arner, R. J.; Krebs, C.; Bollinger, J. M., Jr. *Biochemistry* **2006**, *45*, 5393–5401.
- Xing, G.; Barr, E. W.; Diao, Y.; Hoffart, L. M.; Prabhu, K. S.; Arner, R. J.; Reddy, C. C.; Krebs, C.; Bollinger, J. M., Jr. *Biochemistry* **2006**, *45*, 5402–5412.
- Xing, G.; Diao, Y.; Hoffart, L. M.; Barr, E. W.; Prabhu, K. S.; Arner, R. J.; Reddy, C. C.; Krebs, C.; Bollinger, J. M., Jr. *Proc. Natl. Acad. Sci. U.S.A.* **2006**, *103*, 6130–6135.
- Schweiger, A.; Jeschke, G. *Principles of Pulsed Electron Paramagnetic Resonance*; Oxford University Press: Oxford, U.K., 2001.
- Davoust, C. E.; Doan, P. E.; Hoffman, B. M. *J. Magn. Reson.* **1996**, *119*, 38–44.
- MIOX^{II(III)}– $^2\text{H}_6$ -MI was prepared from the apo protein, as previously described.⁵ The final concentrations were 2.6 mM MIOX, 5.1 mM Fe, 3.4 mM ascorbate, and 100 mM $^2\text{H}_6$ -MI (C/D/N Isotopes, Inc., Quebec, Canada). The concentration of MIOX^{II(III)}– $^2\text{H}_6$ -MI in the sample should have been ~ 1.3 mM.
- Mims Q-band ENDOR spectra were recorded at 2 K on a spectrometer described in ref 8. The ENDOR pattern for a deuteron ($I = 1$) exhibits a $\nu(\pm)$ doublet that is split by the hyperfine coupling, A, and centered at the ^2H Larmor frequency; in principle, these peaks are further split by the quadrupole interaction, P, making the pattern a doublet of doublets, $\nu = |\nu(n) \pm A/2 \pm 3P/2|$.
- DeRose, V. J.; Liu, K. E.; Lippard, S. J.; Hoffman, B. M. *J. Am. Chem. Soc.* **1996**, *118*, 121–134.
- Willems, J.-P.; Lee, H.-I.; Burdi, D.; Doan, P. E.; Stubbe, J.; Hoffman, B. M. *J. Am. Chem. Soc.* **1997**, *119*, 9816–9824.
- Whittington, D. A.; Lippard, S. J. *J. Am. Chem. Soc.* **2001**, *123*, 827–838.
- Modest variations in the metrical values have no significant impact. See Figure S1.
- Barnes, R. G.; Bloom, J. W. *J. Chem. Phys.* **1972**, *57*, 3082–3086.

JA063602C